

IMPACT BEHAVIOR AND OPTIMUM DESIGN OF CFRP/AL HYBRID IMPACT BEAM IN SIDE COLLISION OF AUTOMOBILES

Goichi Ben and Nao Sugimoto

¹ *Dept. of Mechanical Engineering, College of Industrial Technology, Nihon University, 1-2-1, Izumicho, Narashino, Chiba, 275-8575 Japan*

ABSTRACT

Carbon fiber reinforced plastic (CFRP) laminates are used in various industrial fields because they have excellent properties in the specific strength and specific stiffness. The CFRP has a potential of weight reduction in the automotive structure which can contribute to the improvement of mileage as well as the reduction of carbon dioxide. On the other hand, the safety issue in case of collision should be also clarified when employing the CFRP as automotive structures.

In this paper, hybrid beams which consisted of the Al Alloy beam and the CFRP laminate were examined by both experiments and numerical analyses as candidates to replace the conventional steel door guarder beam used inside the automotive door. The experimental relations of impact loading to the displacement for the Al guarder beams with different thicknesses, widths and types of CFRP showed good agreement with those from numerical results. These results show that the numerical method developed here is useful for estimating the impact behavior of CFRP/Al hybrid beams.

Furthermore, the optimum design of hybrid beam was proposed by the developed numerical method here and its usefulness was demonstrated by the experiment.

1. Introduction

It is well known that CO₂ emitted from passenger vehicles is one of major causes of global warming. The most effective method to reduce CO₂ is to produce fuel efficient automobiles. Improvement of the automobile fuel efficiency can be realized by reducing the automobile weight using a lightweight material such as composite materials. Carbon fiber reinforced plastics (CFRP) have been widely used in aerospace industries, industrial goods and other application fields because of their high specific strength and high specific modulus compared with conventional metals. This means that the CFRP can contribute to lightening the weight of automobiles significantly.

Besides reducing the weight, the safety of automobiles is also a very important issue which needs to be investigated along with the reduction of weight. Collision safety of the automobile has been evaluated by full flap frontal crash, offset frontal crash and side impact tests. In the frontal crash, it is possible to absorb the energy by largely deforming the front and the rear parts of automobiles. With increasing interests in reducing the automobile weight and securing the safety of passengers, extensive research has been performed in the recent years for collision impact [1-6].

However, in the side crash, it is hard to absorb the impact energy the same way as the frontal crash, because the survival space of passengers is very narrow. At present, door guarder beams made of steel are used inside the door for absorbing impact energy and their deformation is limited to about 150mm as shown in Fig.1.

thickness (1, 2 and 3mm) were also employed. The effects of these design parameters on the impact energy absorption were examined.

2.2 Experimental method

The 1,000 mm length of hybrid beam was supported by two supportors having a head radius of 15mm and the span between the two supportors was 800 mm. In order to evaluate the capacity of crash energy absorption, a larger size of drop tower facility for the impact test was constructed. The beam received an impact load generated by a free drop mass of 100 kg at an impact speed of 55 km/h. The shape of the impactor was a half cylinder having a 100 mm radius and a 200 mm width and the hybrid beam was fixed by belts to prevent from scattering (Fig.5)

The impact load and the displacement of the impactor were measured by load cells attached to both supportors and by a high-speed camera, respectively.

Table1 Combination of the design parameters.

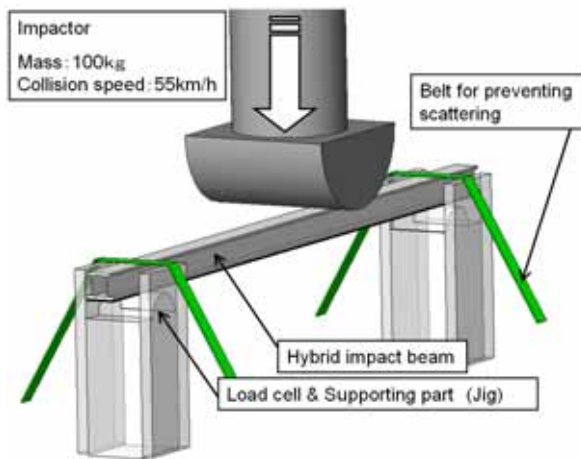


Fig.5 Outline of impact test.

No.	Type of CFRP	Thickness of CFRP [mm]	Width of CFRP [mm]	Type of Adhesive
1	T700S,#2500	1	36	Viscosity
2	T700S,#2500	2	28	High-elongation
3	T700S,#2500	3	20	High-strength
4	M40J,#2500	1	28	High-elongation
5	M40J,#2500	2	20	High-strength
6	M40J,#2500	3	36	Viscosity
7	T800H,#3900-2B	1	36	High-strength
8	T800H,#3900-2B	2	28	Viscosity
9	T800H,#3900-2B	3	20	High-elongation
10	T700S,#2500	1	20	High-elongation
11	T700S,#2500	2	36	High-strength
12	T700S,#2500	3	28	Viscosity
13	M40J,#2500	1	20	Viscosity
14	M40J,#2500	2	36	High-elongation
15	M40J,#2500	3	28	High-strength
16	T800H,#3900-2B	1	28	High-strength
17	T800H,#3900-2B	2	20	Viscosity
18	T800H,#3900-2B	3	36	High-elongation

2.3 Results of experiments

18 specimens with combining the design parameters were fabricated and tested. Their specifications are listed in Table 1. Among all the specimens, No.18 specimen absorbed the largest impact energy is shown in Fig.6. The design parameters of this specimen were high elongation adhesive, the thickness of 3mm and width of 36mm of T800 CFRP, respectively. The absorbed impact energy until the displacement of 150mm was 1827J. This value was somewhat higher or almost same as that of the steel door guarder beam. After the impact load reached to the maximum value of 24.0kN at the earlier time of impact, it soon recovered to the almost same value because of the effects of CFRP reinforcement. The center of unidirectional CFRP laminate broke at the displacement of 126 mm and the impact load became to zero at the displacement of 164mm. Fig.7 shows the fiber broke mode of CFRP.

On the other hand, Fig.8 shows the impact test results of No.12 specimen. This specimen could not absorb the larger impact energy and its value was 1493J. This reason was that the CFRP laminate came off the surface of Al beam because the

breakage of adhesive was faster than that of CFRP laminate. Fig. 9 shows the breakage of adhesive and CFRP laminate delaminated from the Al beam.

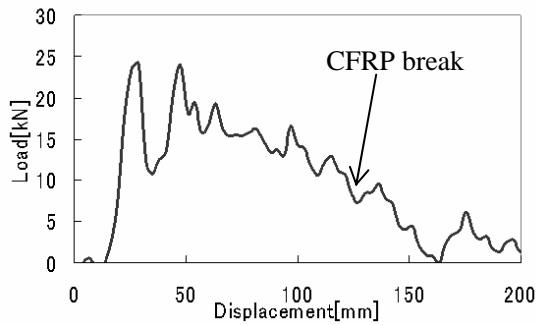


Fig.6 Displacement-load curve of No.18 specimen.

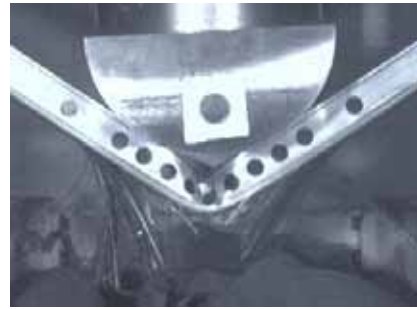


Fig.7 Break of CFRP laminates. (Specimen No. 18)

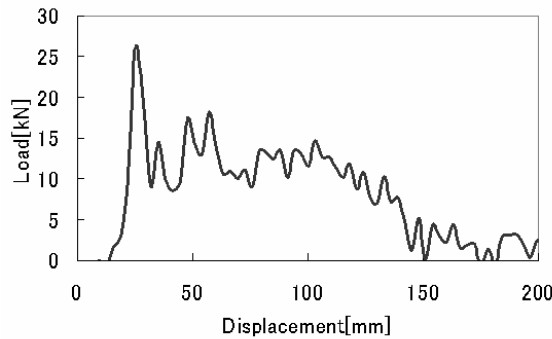


Fig.8 Displacement-load curve of No. 12 specimen.



Fig.9 Breakage of Adhesive laminates.(Specimen No.12)

3. Impact response analysis by F.E.M.

3.1 Analytical model

In the numerical analysis, a dynamic explicit FEM solver (PAM-CRASH Solver2006) was employed. The analytical model was created based on the size of the specimens, impactor and the support parts in the test. The analysis model is shown in Fig.10. The elastic-plastic shell element (MAT103) for the Al beam part and the unidirectional composite global ply shell element (MAT131, ITYP=1) for the CFRP laminate were used, respectively. The impactor and the supporters were modeled as a rigid body. The mass of 100kg and an initial velocity of 55km/h was given to the impactor. The total node number was 21,583 and the total element number was 19,504.

The contact element between the impactor and the upper surface of hybrid CFRP/Al beam and between the supporter and the lower surface of hybrid CFRP/Al beam was Contact Type 33 with the friction and penalty coefficients of 0.17 and of 0.1, respectively. For the interface of Al beam and the CFRP laminate, “Link Material 303” was used for modeling adhesion of interface.

Table 2 shows the material properties of the aluminum alloy and Fig.11 shows its true strain-true stress curve. Table 3 shows the material properties of three kinds of Adhesive and Table 4 shows the material properties of three kinds of CFRP.

For the failure criterion of Al beam element, a 5% decrease of thickness in the tension state or an increase 30% of thickness in the compression state was used. Next, the failure criteria of adhesive and CFRP laminate were employed “Fracture energy of

mode 1 and mode 2 of Link Material 303” and the maximum stress theory, respectively. When the value of the element was over these criteria, it was deleted in the succeeding FEM calculation.

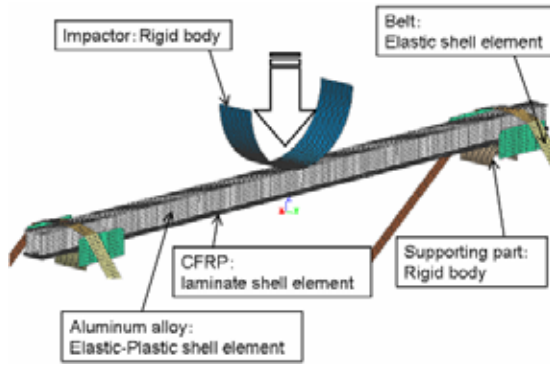


Fig.10 F.E.M. Analytical Model.

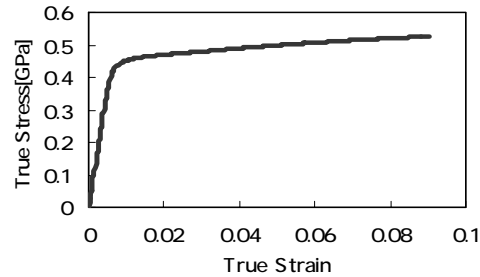


Fig.11 True Strain-True stress curve of aluminum alloy.

Table2 Material properties of aluminum alloy.

Aluminum Alloy	Tensile Strength [MPa]	Yield Stress [MPa]	Elastic Modulus [GPa]	Poisson Ratio
Z6W-T5	480	412	70	0.33

Table3 Material properties of adhesive.

Type of Adhesive	σ_{max} [MPa]	E [GPa]	τ_{max} [MPa]	G [GPa]
High-strength	30	3	25	1.15
High-elongation	10	0.36	10	0.138
Viscosity	1	0.1×10^{-4}	1	0.038×10^{-4}

Table4 Material properties of CFRP.

CFRP	F_L [MPa]	E_L [GPa]	F_T [MPa]	E_T [GPa]	F_{LT} [MPa]	G_{LT} [GPa]	ν_{LT} [MPa]
T700S,#2500	2550	135	69	8.5	98	4.4	0.34
T800H,#3900-2B	2840	160	80	7.8	98	4.4	0.34
M40J,#2500	2450	230	53	7.7	59	3.9	0.27

3.2 Comparison of Experimental and FEM results

Fig 12 shows both impact load to displacement curves obtained by the experiment and the FEM for the No. 18 specimen which absorbed the highest impact energy. Both results showed the almost same impact behavior and the absorbed impact energy obtained by the FEM was 1822J and the error of impact energy was 0.27% to the experimental one. Fig.13 compares the failure mode of hybrid beam and two results showed the same breakage of CFRP laminate at the center of hybrid beam.

In order to demonstrate the effectiveness of FEM method developed here for estimating the impact behavior of hybrid CFRP/Al beam, the result of No.12 specimen which showed the breakage of adhesive, not the breakage of CFRP laminate, was compared with that obtained by FEM. Fig 14 expresses a good agreement of the load-displacement relation except the value of initial peak of load and the error of absorbed impact energy was 7% between both results.

Fig. 15 shows the failure mode obtained two results and the CFRP laminate came off the Al beam in both cases because of the breakage of adhesive. The failure mode of other specimens listed Table 5 showed the mixture of both breakages of CFRP laminate and adhesive. Table 5 lists the impact energy absorption for all of the specimens except No.5 and No. 8 specimens owing to the miss of experiment.

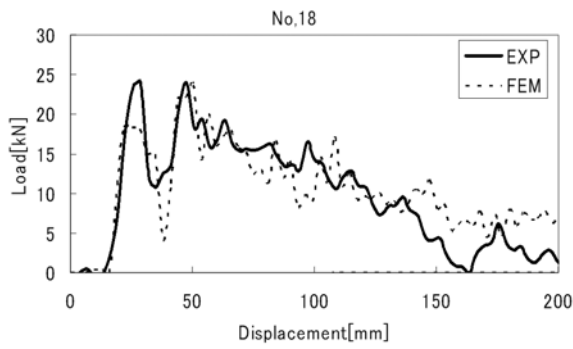


Fig.12 Comparison of experimental result with F.E.M. one. (Specimen No. 18)

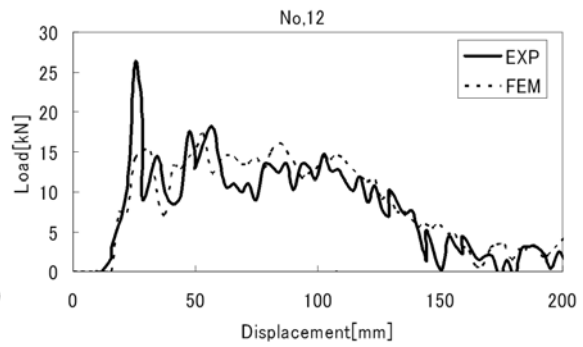


Fig.14 Comparison of experimental result with F.E.M. one. (Specimen No. 12)

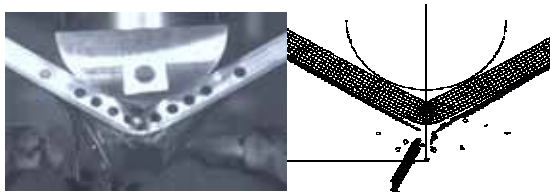


Fig.13 Comparison of experimental fracture mode with F.E.M one. (Specimen No. 18)

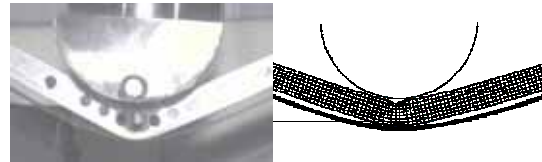


Fig.15 Comparison of experimental fracture mode with F.E.M one. (Specimen No. 12)

Table5 Impact energy absorption for all specimens.

No.	Type of CFRP	Thickness of CFRP [mm]	Width of CFRP [mm]	Type of Adhesive	Break mode	Absorbed energy in Experiment [J]	Absorbed energy in Analysis [J]	Error[%]
1	T700S,#2500	1	36	Viscosity	Fiber break	1345	1384	2.90
2	T700S,#2500	2	28	High-elongation	Fiber break	1342	1358	1.19
3	T700S,#2500	3	20	High-strength	Delamination	1605	1685	4.98
4	M40J,#2500	1	28	High-elongation	Fiber break	1531	1529	0.13
5	M40J,#2500	2	20	High-strength	—	—	—	—
6	M40J,#2500	3	36	Viscosity	Fiber break	1583	1574	0.59
7	T800H,#3900-2B	1	36	High-strength	Fiber break	1626	1737	6.83
8	T800H,#3900-2B	2	28	Viscosity	—	—	—	—
9	T800H,#3900-2B	3	20	High-elongation	Delamination	1371	1470	7.22
10	T700S,#2500	1	20	High-elongation	Fiber break	1549	1595	2.97
11	T700S,#2500	2	36	High-strength	Fiber break	1570	1627	3.63
12	T700S,#2500	3	28	Viscosity	Delamination	1487	1591	6.99
13	M40J,#2500	1	20	Viscosity	Fiber break	1322	1430	8.17
14	M40J,#2500	2	36	High-elongation	Fiber break	1815	1748	3.69
15	M40J,#2500	3	28	High-strength	Fiber break	1569	1663	5.99
16	T800H,#3900-2B	1	28	High-strength	Fiber break	1667	1692	1.50
17	T800H,#3900-2B	2	20	Viscosity	Delamination	1636	1613	1.41
18	T800H,#3900-2B	3	36	High-elongation	Fiber break	1827	1822	0.27

The No.18 specimen which absorbed the largest impact energy, consisted of 3mm thickness and 40mm width of T800 and the high elongation adhesive. The average error of impact energy absorption for all of the specimen was 3.65% between the experimental and FEM results.

4. Optimum design by F.E.M.

In order to obtain the larger impact energy absorption, the design parameters were changed in the numerical simulation of FEM method because of confirming the effectiveness of this method developed here through the comparison of both results. First, the sort of CFRP was examined while remaining other design parameters. Next, the cross section of Al beam was changed under the condition of keeping same area.

4.1 Comparisons of three kinds of CFRP

In the experiment, the No.18 specimen used T800 CFRP absorbed the largest impact energy. However, the specimens having the CFRP laminate of T700 or M40 and the other same design parameters as the No.18 specimen were not fabricated. Therefore, the two hybrid beams having the CFRP laminate of T700 and M40 were calculated by the FEM method

Fig. 20 compares three results of specimens with T800, T700 and M40. The result of T700 showed the highest first peak of impact load and the largest impact energy absorption until the displacement of 150mm. Its value was 1863J and an increase of 41J was obtained than the case of T800.

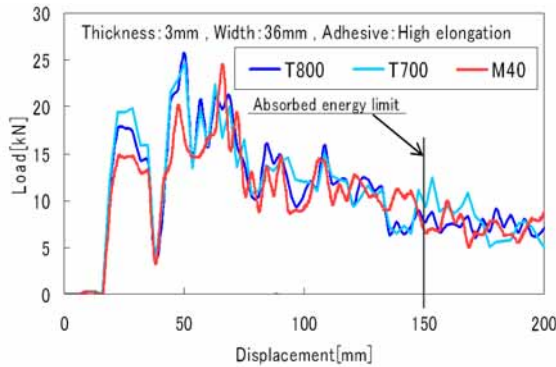


Fig.16 Displacement-load curves of three kinds of hybrid beams with different CFRP.

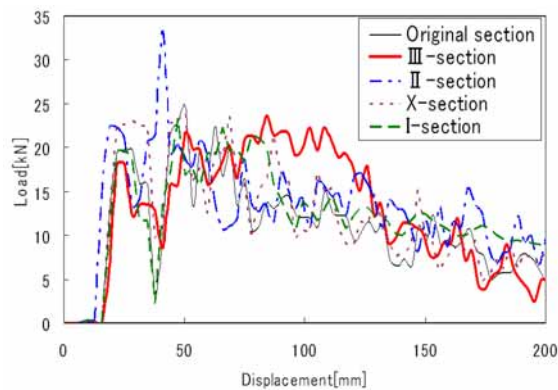


Fig.19 Comparisons of displacement-load curves for five hybrid beams .

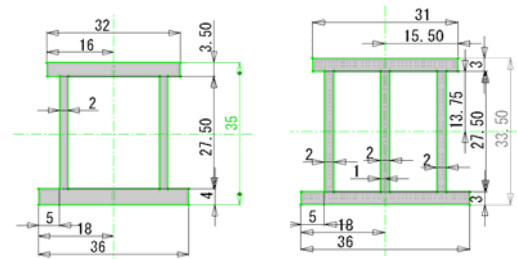


Fig.17 Cross section of Original Beam.

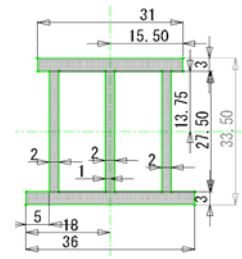


Fig.18a Cross section of Beam.

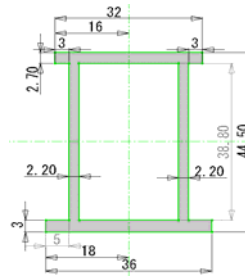


Fig.18 b Cross section of Beam.

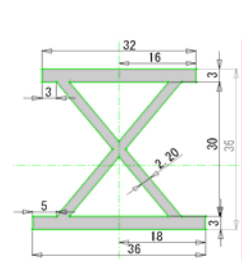


Fig.18 c Cross section of Beam.

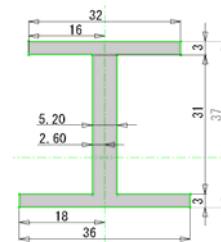


Fig.18d Cross section of Beam.

Although, the largest strength of CFRP is T800 and the largest Young's modulus of E_L is M40 in Table 4, the result of T700 was the most proper CFRP among three CFRPs. In the hybrid of CFRP/Al beam, the CFRP was not necessarily required the larger strength nor the larger Young's modulus. The most important properties of CFRP were the proper strength and Young's modulus to be able to follow the deformation of Al beam.

4.2 Design of Al beam cross-sections

Next the cross section shape of Al beam was changed as a design parameter in order to increase the impact energy absorption. Here, the thickness of 3 mm and the width of 36 mm of T700 CFRP and the adhesive of high elongation type were employed in the numerical simulation of FEM. The area of cross section of Al beam used in the experiment (called as the original section) was 366 mm^2 as shown in Fig. 17 and the four kinds of cross section shape as shown in Figs. 18a-d were devised under the condition of keeping the same area as that of the original beam.

The vertical member of the cross-section in Fig. 18a was increased from 2 to 3 by reducing the thickness of the horizontal members and it was called _1 beam. Fig. 18b shows the higher vertical members compare with those of the original beam aiming larger second moment of area and it called as _2 beam. In Fig. 18c, two vertical members were crossed each other and it was called as _3 beam. Finally, one thicker vertical member was connected to the upper and the lower horizontal members (Fig. 18d) and it was called as _4 beam.

The displacement-load curves of four hybrid beams having the devised each cross section of Al beam were compared with that of original hybrid beam in Fig. 23. Among them, the _1 section showed the highest impact load at the earlier time of impact and the _4 section presented the larger and constant impact load (about 20kN) until the displacement of 120mm.

The impact energies of absorption for the hybrid beams with the _1 , _2 and _3 sections were 2245J, 2171J and 2056J, respectively. They were larger than 1822J of the original hybrid beam except the hybrid beam with the _4 section. The absorbed impact energy of the hybrid beam with the _1 section was 23% larger than that of the original one.

4.3 Comparison of Experimental and FEM results for _1 Beam.

In order to confirm the performance of _1 Beam proposed in the FEM analysis, three prototype (Fig. 20) of _1 beams were fabricated and their experiments were executed. Fig. 21 shows the comparison of three experimental load-displacement curves with that of FEM. The FEM curve showed the good agreement with three experimental curves and the average of experimental absorbed energy was 2119J. The error between the experiment and the FEM was 5.6%.

Fig. 22 shows failure mode obtained one of the experiment and the FEM and they also showed good agreement.

Conclusions

1. The CFRP/Al hybrid door guarder beam showed an excellent performance of absorbing impact energy and its maximum displacement after the impact was smaller than that of steel one.
2. The CFRP/Al hybrid beam with the thicker CFRP showed the larger impact failure displacement of hybrid beam because its fracture was extended by the thicker CFRP and then it absorbed more impact energy.

3. From the comparison of FEM results with the experimental ones for specimens of CFRP/Al hybrid beams, the proposed numerical method was found to be very useful for analyzing the hybrid beams.

4. The change of cross section of Al beam increased the impact energy absorption by the numerical simulation and three experimental results verified the larger impact energy absorption. Therefore, changing the design parameters of the hybrid beam may result in further increase of impact energy absorption



Fig.20 Prototype of beam.

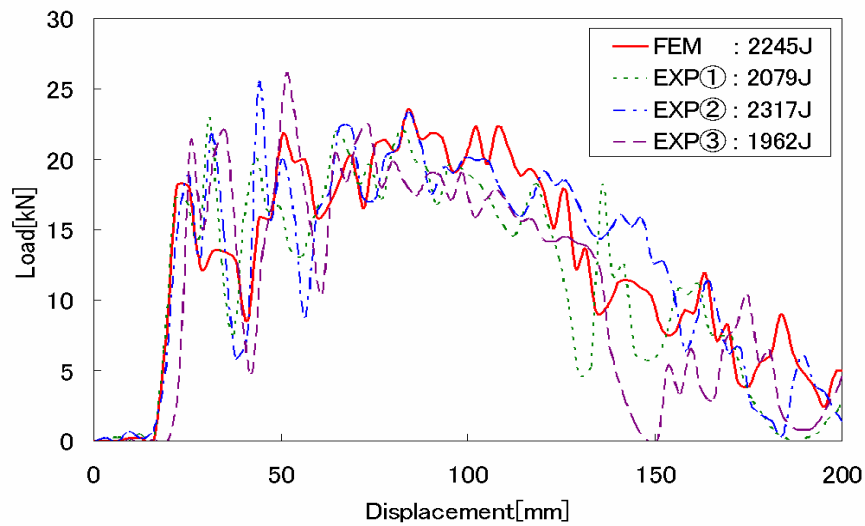


Fig.21 Comparison of experimental and FEM results for beam)

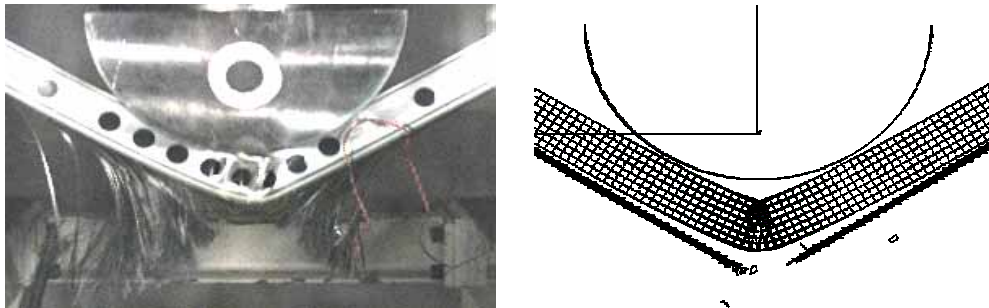


Fig.22 Comparison of Fracture Mode obtained both results

ACKNOWLEDGEMENTS

This study was conducted as part of the Japanese National Project R&D of Carbon Fiber-Reinforced Composite Materials to Reduce Automobile Weight supported by NEDO (the New Energy and Industrial Technology Development Organization) and the authors acknowledge the assistance of Toray Industries, Inc. who supplied the materials for these test specimens.

REFERENCES

1. P.K. Mallick and L.J. Broutman, *J. Testing and Evaluation*, 5, 190 (1977)
2. S.S. Cheon, T.S. Lim and D.G. Lee, *Comp Struct*, 46, 267 (1999)
3. D.G Lee, T.S. Lim and S.S. Cheon, *Comp Struct*, 50, 381 (2000)
4. G. Ben, T. Uzawa, H.S. Kim, Y. Aoki, H. Mitsuishi and A. Kitano, *Transaction of JSME Series A*, 70(694), 824 (2004) (in Japanese)
5. A. G. Caliska, *Proceedings of IME2002, ASME, International Mechanical Engineering Congress & Exposition(2002)*
6. H.S.Kim, G.Ben and Y.Iizuka, *Proceedings of 11th Japan -US Conference of Composite Materials (2004)*
7. G.Ben, Y.Aoki and H.S.Kim, *Proceedings of 12th US-Japan Conference on Composite Materials (2006)*.
8. G.Ben , Y.Aoki and N.Sugimoto, *Proceedings of 16th ICCM, (2007,CD-ROM File name: "FrFM-02")*